OCS Study
BOEM 2020-012

Pacific Continental Shelf Environmental Assessment (PaCSEA): Characterization of Seasonal Water Masses within the Northern California Current System Using Airborne Remote Sensing off Northern California, Oregon, and Washington, 2011–2012

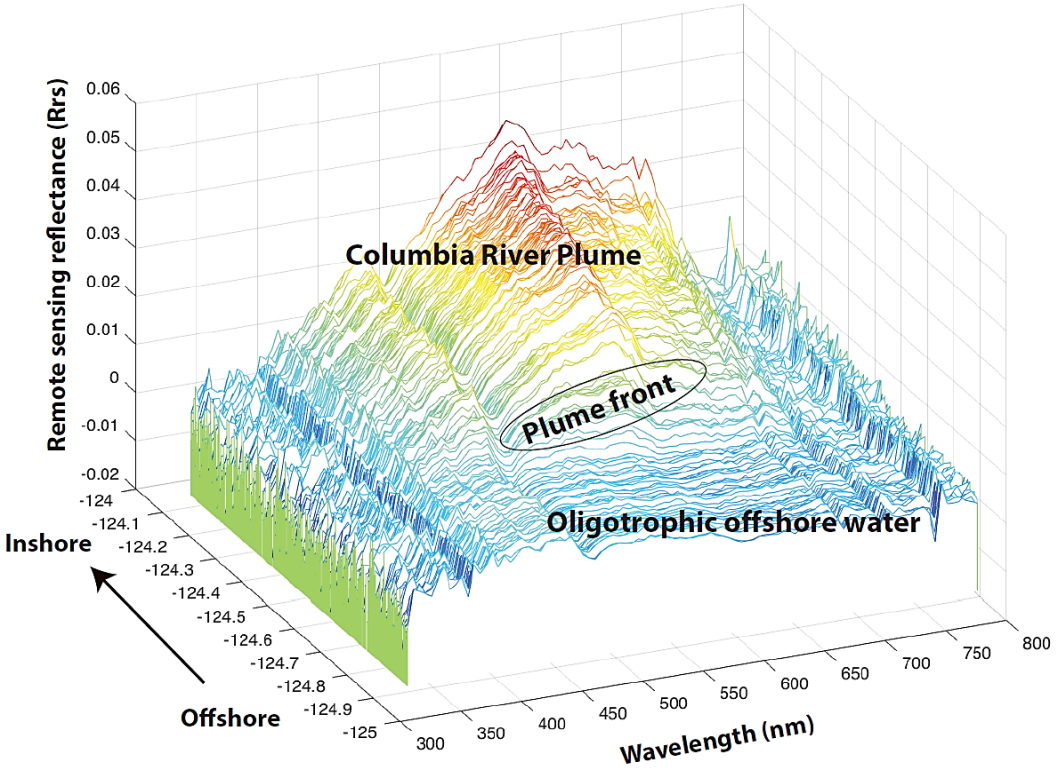

US Department of the Interior
Bureau of Ocean Energy Management
Pacific OCS Region

BOEM
Bureau of Ocean Energy Management

OCS Study
BOEM 2020-012

Pacific Continental Shelf Environmental Assessment (PaCSEA): Characterization of Seasonal Water Masses within the Northern California Current System Using Airborne Remote Sensing off Northern California, Oregon, and Washington, 2011–2012

February 2020

Authors:
Jennifer A. Schulien
Josh Adams
Jonathan J. Felis

Prepared under Intra-Agency Agreement M10PG00081
By
U.S. Department of the Interior
U.S. Geological Survey
Western Ecological Research Center
Santa Cruz Field Station
2885 Mission Street
Santa Cruz, CA 95060

US Department of the Interior
Bureau of Ocean Energy Management
Pacific OCS Region

BOEM
Bureau of Ocean Energy Management

DISCLAIMER

This study was funded, in part, by the U.S. Department of the Interior, Bureau of Ocean Energy Management (BOEM), Environmental Studies Program, Washington, DC, through Intra-Agency Agreement Number M10PG00081 with the U.S. Geological Survey (USGS). This report has been technically reviewed by BOEM, and it has been approved for publication. This product has been peer reviewed and approved for publication consistent with USGS Fundamental Science Practices (http://pubs.usgs.gov/circ/1367/). Any use of trade, firm, or product names is for descriptive purposes only and does not imply endorsement by the U.S. Government.

REPORT AVAILABILITY

To download a PDF file of this report, go to the U.S. Department of the Interior, Bureau of Ocean Energy Management Data and Information Systems webpage (http://www.boem.gov/Environmental-Studies-EnvData/), click on the link for the Environmental Studies Program Information System (ESPIS), and search on 2020-012. The report is also available at BOEM's Recently Completed Environmental Studies - Pacific webpage (https://www.boem.gov/Pacific-Completed-Studies/).

CITATION

Schulien, JA, Adams, J, Felis, J. 2020. Pacific Continental Shelf Environmental Assessment (PaCSEA): Characterization of Seasonal Water Masses within the Northern California Current System Using Airborne Remote Sensing off Northern California, Oregon, and Washington, 2011–2012. Camarillo (CA): U.S. Department of the Interior, Bureau of Ocean Energy Management, Pacific OCS Region. OCS Study BOEM 2020-012. 26 p.

ABOUT THE COVER

Cover image: Remote sensing reflectance hyperspectrograph for PaCSEA Transect 29 depicting a bimodal, tidal river plume off the Colombia River, Washington, January 2011. Courtesy of Jennifer Schulien (USGS).

ACKNOWLEDGMENTS

This project was funded by the Bureau of Ocean Energy Management through Intra-Agency Agreement M10PG00081 with the U.S. Geological Survey (USGS) Western Ecological Research Center (WERC). Greg Sanders (BOEM) helped initiate the study and provided constructive advice. David Pereksta (BOEM) provided contract oversight. Low-elevation aerial survey methods were reviewed by the National Oceanic and Atmospheric Administration, National Marine Fisheries Service, who granted a Letter of Concurrence (4 January 2011) accepting USGS mitigation measures to avoid marine mammal disturbance. Jennifer Schulian was supported by USGS-WERC and gives special thanks to P. Raimondi (University of California, Santa Cruz) and J. Ryan (Monterey Bay Aquarium Research Institute). We thank the Kudela Lab, especially Sheri Palacios, and Raphe Kudela, and Stephanie Flora (Moss Landing Marine Labs) for assistance with programing. David Johncox (USGS) provided consultation regarding special-use aerial operations safety and the Department of the Interior's Interagency Aviation Training program provided useful training in advance of safe aerial operations. We are especially grateful to the pilots at Aspen Helicopters (Oxnard, California) and Gold Aero (Arlington, Washington) for their expert ability to conduct safe operations at low elevation, often far from land—over the open ocean.

Contents

List of Figures ii

List of Tables iii

List of Abbreviations and Acronyms iv

1 Introduction 1

1.1 Study region, oceanography, and ecology 1

2 Methods 4

2.1 Aerial surveys and aircraft remote sensing 4

2.2 Environmental remote sensing 4

2.3 Additional environmental data 7

2.4 K-means cluster analysis 7

3 Results and discussion 7

3.1 Aerial survey effort 7

3.2 Remote sensing 8

3.2.1 Airborne HR3 matchups with MODIS satellite data 13

3.3 K-means clustering analysis 14

3.3.1 Winter surveys 14

3.3.2 Summer surveys 17

3.3.3 Autumn surveys 19

4 Summary and conclusion 21

5 References 21

List of Figures

Figure 1. Remote sensing reflectance hyperspectograph over the CRP region 2
Figure 2. Survey aircraft 3
Figure 3. Study area 5
Figure 4. Survey area, Columbia River flow, and winds 6
Figure 5. Sea surface temperature 10
Figure 6. Monthly MODIS satellite imagery 11
Figure 7. Chlorophyll a concentrations derived from HydroRad3 ocean color 12
Figure 8. MODIS satellite remote-sensing matchups with HydroRad3 13
Figure 9. K-means results for winter surveys 16
Figure 10. K-means results for summer surveys 18
Figure 11. K-means results for autumn surveys 20

List of Tables

Table 1. Summary of low-elevation aerial survey effort (linear km surveyed) during PaCSEA surveys 8

Table 2. Airborne flights with concurrent environmental data 9

Table 3. Summary of k-means clustering results 15

List of Abbreviations and Acronyms

Au	Absorbance units
BOEM	Bureau of Ocean Energy Management
Chla	Chlorophyll *a*
CCS	California Current System
NCCS	Northern California Current System
a_{CDOM}	absorption of Colored Dissolved Organic Matter CRP Columbia River Plume
°C	Degrees Celsius
GPS	Global Positioning System
h	Hour
HR3	HyrdoRad3
km	Kilometers
L_d	Downwelling Radiance
E_d	Downwelling Irradiance
L_u	Upwelling Radiance
${}_nL_w$	Normalized water-leaving radiance
m	Meters
MODIS	Moderate Resolution Imaging Spectroradiometer
NASA	National Aeronautical and Space Administration
NOAA	National Oceanic and Atmospheric Administration
nm	Nanometers
NM	Nautical Miles
NPP	Net Primary Production
OWEI	Offshore Wind Energy Infrastructure
OCS	Outer Continental Shelf
PaCSEA	Pacific Continental Shelf Environmental Assessment
Rrs	Remote Sensing Reflectance
SST	Sea Surface Temperature
s	Second
USGS-WERC	U.S. Geological Survey-Western Ecological Research Center
W	Watts

1 Introduction

Interest in developing renewable energy in the ocean has recently increased, some of which will include power generation infrastructure and support activities located within continental shelf (and potentially deeper) waters off the U.S. Pacific coast, beyond state waters (i.e., outside three nautical miles [NM]). The Bureau of Ocean Energy Management (BOEM) is currently considering renewable energy proposals off the coast of Oregon, California, and Hawaii (BOEM 2017). The 2011–2012 USGS Pacific Continental Shelf Environmental Assessment study (PaCSEA, Adams et al., 2014) was intended to provide up-to-date information on species composition, distribution, abundance, seasonal variation, and habitat utilization among marine birds and mammals on the outer continental shelf (OCS) within a broad region of the northern California Current System (NCCS; herein, the region between Fort Bragg, California [39.3°N] to Grays Harbor, Washington [47°N]). The NCCS supports abundant populations of seabirds and marine mammals, but comprehensive aerial surveys have not been conducted during certain months (e.g., winter) or were conducted two to four decades ago. Briggs et al., (1987) conducted extensive low-elevation surveys for marine birds and mammals off central and northern California from February 1980 through January 1983, and Bonnell et al., (1992), Briggs et al., (1992), and Green et al., (1992) conducted similar, extensive aerial surveys from April 1989 to September 1990 off Oregon and Washington. Suryan et al., (2012) provided a review of surveys conducted off Oregon and a similar effort also gathered existing seabird abundance data off Washington to create species distribution models using environmental predictors (Menza et al., 2016). *In situ* sensing of the ocean environment in the aerial surveys prior to PaCSEA was limited to sea surface temperature (SST) measured with pyrometry and composite imagery of the ocean collected via earth-orbiting satellites.

Our three primary objectives for PaCSEA were to (1) conduct aerial at-sea surveys of seabirds and marine mammals in shelf and slope waters off northern California, Oregon, and Washington and summarize species and seasonal at-sea densities, (2) conduct a comparison with existing similar surveys in northern California, Oregon, and Washington, and (3) validate and enhance aerial survey data for numerically abundant indicator species and certain resident breeding and non-resident migratory seabird species. Objective 1 included enhancing *in situ* remote sensing of the ocean by including a hyperspectral radiometer to collect continuous, ocean color data during surveys. Data generated using remote sensing were intended to assist resource managers in the evaluation of proposed renewable energy sites and environmental review of specific project proposals received by BOEM. In addition, new data regarding seabird density distributions along with data on environmental factors will enhance continuing efforts to apply predictive modeling for (1) species distributions (Nur et al., 2011; see also, Data Synthesis and High-resolution Predictive Modeling of Marine Bird Spatial Distributions on the Pacific OCS [BOEM PC-15-01]) and (2) applied vulnerability assessments among seabirds in the CCS to offshore wind energy infrastructure (OWEI; Adams et al., 2016, Kelsey et al., 2018). Here, we report sea surface temperature, derived ocean color chlorophyll *a* (Chla), absorption by colored dissolved organic matter (a_{CDOM}), proxy particle load, and statistically-derived water mass classifications for all surveys flown during the 2011–2012 PaCSEA study.

1.1 Study region, oceanography, and ecology

The California Current System (CCS) is an eastern boundary current spanning the region from Baja California, Mexico to British Columbia, Canada and extending up to 1,000 km offshore (Huyer 1983, Miller et al., 1999). Despite a poleward decrease in wind-driven Ekman transport, surface concentrations of Chla increase with latitude (Ware and Thomson, 2005). Intermittent upwelling with periods of

relaxation occur at time scales of 2–10 days (coincident with time-scales of phytoplankton blooms). Frontal boundaries related to the Columbia River, submarine canyons that enhance coastal upwelling, internal waves generated by remote winds, broad continental shelves, and coastlines without capes (and associated local bathymetry) make the NCCS one of the most productive areas within the CCS (Hickey and Banas, 2008; Hickey et al., 2006).

The Columbia River plume (CRP) is one of the most important habitat features in the NCCS, supplying 77% of the total freshwater discharge from San Francisco, California to the Strait of Juan de Fuca, Washington (Hickey et al., 1998). The CRP also is a major source of dissolved and particulate organic material, nutrients, and trace metals to the NCCS (Hickey et al., 2005; Aguilar-Islas and Bruland, 2006). Although the Columbia River has relatively low iron concentrations compared with other rivers in the U.S. and is not a major source of nitrogen to the region (nitrogen is primarily utilized in the estuary before entering the Pacific Ocean), upwelling and re-suspension of estuarine sediments during low tide supply enough iron such that nitrogen ultimately limits phytoplankton growth in the region (Bruland et al., 2008; Kudela and Peterson, 2009). The Columbia River provides important nutrients to support marine productivity, especially during periods of weak upwelling (Kudela et al., 2010).

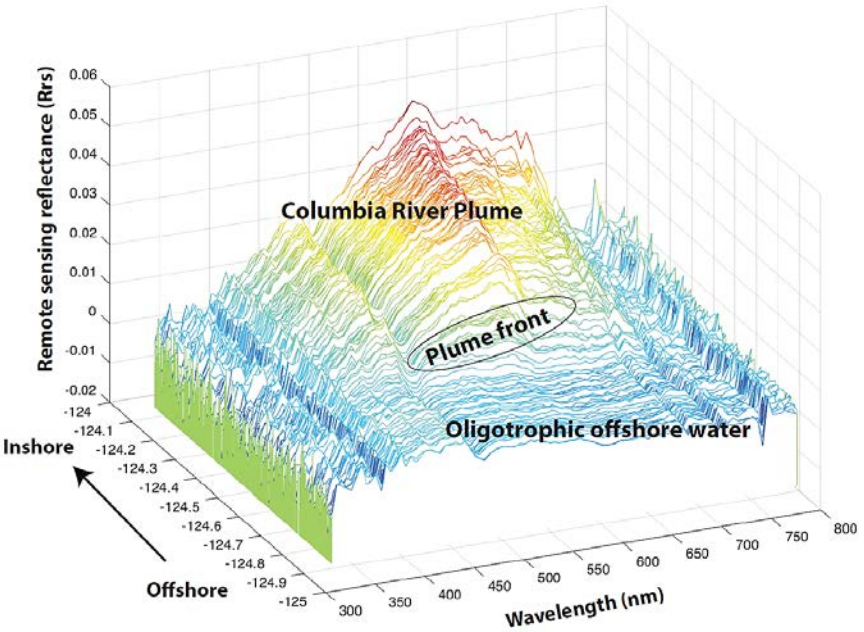

Figure 1. Remote sensing reflectance hyperspectograph over the CRP region
Example of along-transect (#29, Columbia River line) hyperspectrograph of remote sensing reflectance (Rrs) collected from an aircraft-mounted radiometer during survey of the Columbia River. Plume water is easily detectable and contrasts markedly with offshore oligotrophic waters of the inner California Current.

Elevated net primary production (NPP) in this region fuels transfer of energy to higher trophic levels (Kudela et al., 2010). Zooplankton biomass is enhanced within ‘aged’ plume water and concentrated along strong density gradients within the plume’s pycnocline and at the plume boundary (Peterson and Peterson, 2008). South of the CRP, approximately 55-km offshore of Oregon (44°N, 125°W), Heceta Bank is another ‘hotspot’ in the NCCS where a unique biochemical environment promotes high phytoplankton NPP (Hickey and Banas, 2003). Both the CRP and Heceta Bank also support diverse and abundant mesopredators including fishes, seabirds, and marine mammals and are particularly important

when normal conditions change and the subsequent nutrient flux is reduced (i.e., during El Niño events; Ainley et al., 2005; Adams et al., 2012, Zamon et al., 2014). Many fisheries, including Pacific salmon (*Onchyrinchus* spp.), northern anchovy (*Engraulis mordax*), and Pacific sardine (*Sardinops sagax*), exist along the coast, making effective management of coastal and marine resources in the NCCS both ecologically and economically important. To inform management and marine spatial planning, classification of regions of similar water properties over appropriate spatial scales may provide useful descriptions of species habitats (Longhurst et al., 1995; Devred et al., 2007) and help efforts to better predict species distributions (Louzao et al., 2012) and species abundances at sea (Menza et al., 2016).

Here, we use ocean color measurements (Figure 1) and sea surface temperature (SST) data collected with sensors mounted on low-flying aircraft to characterize NCCS water masses and identify patterns among seasons and between years. To accomplish this, we applied k-means clustering to measured and derived ecologically-relevant physical and bio-optical variables (SST, Chla, absorbance by colored dissolved organic matter [a_{CDOM}], proxy particle load). These classifications will be used in the future to evaluate species habitat distributions in the NCCS.

Figure 2. Survey aircraft
Survey aircraft used during the PaCSEA program. Partenavia P-68 Observer (left; Aspen Helicopters, Oxnard, CA) and Commander AC-500 (right; GoldAero, Arlington, WA). Photo courtesy J. Felis, USGS.

2 Methods

2.1 Aerial surveys and aircraft remote sensing

We conducted six low-altitude aerial surveys (twin-engine, fixed, high-wing aircraft: Partenavia P-68, Aspen Helicopters, Oxnard, California, or Commander AC-500, GoldAero, Arlington, Washington; Figure 2). We flew 32 east-west-oriented uniform transects (spaced at 15′ latitude [27.8-km] intervals) when possible to the 2000-m isobath (includes shelf, slope, and rise waters) to ensure comparable spatial and temporal coverage with similar historic datasets. The primary survey area extended from Fort Bragg, California (39.3°N) to Grays Harbor, Washington (47°N) and focused on federal waters outside of the 3-mile boundaries (Figure 3). We designed our at-sea surveys so they would be comparable with historic transect lines off northern California (Briggs et al., 1987) and off Oregon and Washington (Briggs et al., 1992). We included six focal-area surveys nested within the overall broad transect survey area at the request of BOEM (Figure 3). Each focal-area survey consisted of ten, 25-km long, parallel transect lines targeting shelf waters and spaced at 6-km intervals. This pattern (broad survey lines and focal-area survey lines) was surveyed during each of three oceanographic seasons: summer during upwelling (23–30 June 2011 and 1–5 July 2012), autumn during upwelling/relaxation (7–19 October 2011 and 19–24 September 2012), and winter during downwelling (14–26 January 2011 and 17–27 February 2012). Aerial survey methods follow Mason et al. (2007) with slight modifications. Surveys were flown at 160 km h^{-1}, and we used a Global Positioning System (GPS) unit linked to a laptop computer that allowed us to simultaneously collect coordinates (WGS-84 map datum), sea surface temperature (SST, degrees Celsius [°C]) determined via a belly-mounted pyrometer, and ocean color data via an onboard radiometer. Remote sensing data were collected simultaneously with seabird abundance and distribution observations (see Adams et al., 2014).

2.2 Environmental remote sensing

Raw HydroRad3 (HR3; HOBI Labs, Bellevue, Washington) measurements of downwelling irradiance (E_d), downwelling radiance (L_d), and upwelling radiance (L_u) were first calibrated and processed to full engineering units using manufacturer-supplied calibration constants (RadSoft Version 1.1, HOBI Labs, Inc., Bellevue, Washington). These data were imported into Matlab (Version 2011a Student; MathWorks, Natick, MA) and attributed with GPS flight data (geographic coordinates) based on date and time. Full hyperspectral data (0.3-nm intervals) then were reduced to 5-nm intervals using linear interpolation. We distinguished spikes representing bad data from very high real values by examining gradients between sequential points.

The downwelling irradiance (E_d) was multiplied by 0.97 following Doxaran et al. (2012) to account for air-sea transmittance and Fresnel reflection. The upwelling radiance (L_u) was divided by 0.54 to account for the partial reflection and transmission of the upwelled radiance through the sea surface (Mobley 1999). We corrected L_u for sun angle and calculated water-leaving radiance ($_nL_w$) according to Gordon and Voss (1999). Because the survey aircraft were flown at low altitude (60-m ASL), absorption and scattering in the atmosphere were assumed to be negligible. We calculated remote-sensing reflectance (R_{rs}) according to the SeaWiFS Optics Protocol (Mueller et al., 2003). Chla was calculated using the CALFIT algorithm (Kahru et al., 2012), which is an optimization of the fourth-order polynomial coefficients of the OCv-type chlorophyll algorithms refined for use in the CCS. Absorbance by CDOM (a_{CDOM}) was estimated using the algorithm originally developed for use with Sea-Viewing Wide Field-of-View Sensor (SeaWiFS) data (Kahru and Mitchell, 2001). The normalized water-leaving radiance at 555 nm ($_nL_w$[555], scaled 0–1.0) was used as proxy particle load (Otero and Siegel, 2004).

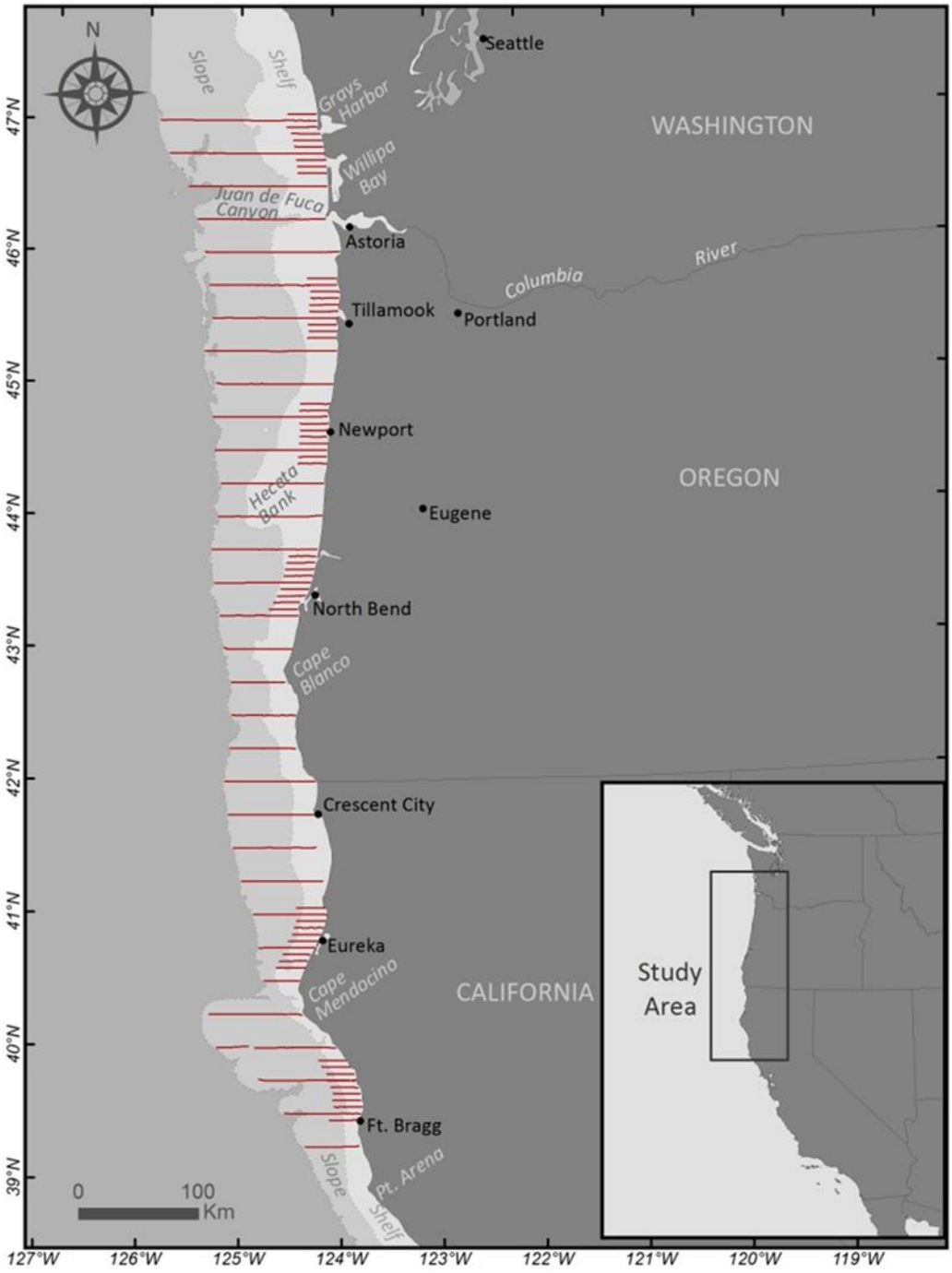

Figure 3. Study area
Pacific Continental Shelf Environmental Assessment (PaCSEA) study area showing 32 broad transects, six focal-area transect zones, and geographic place names referenced in text.

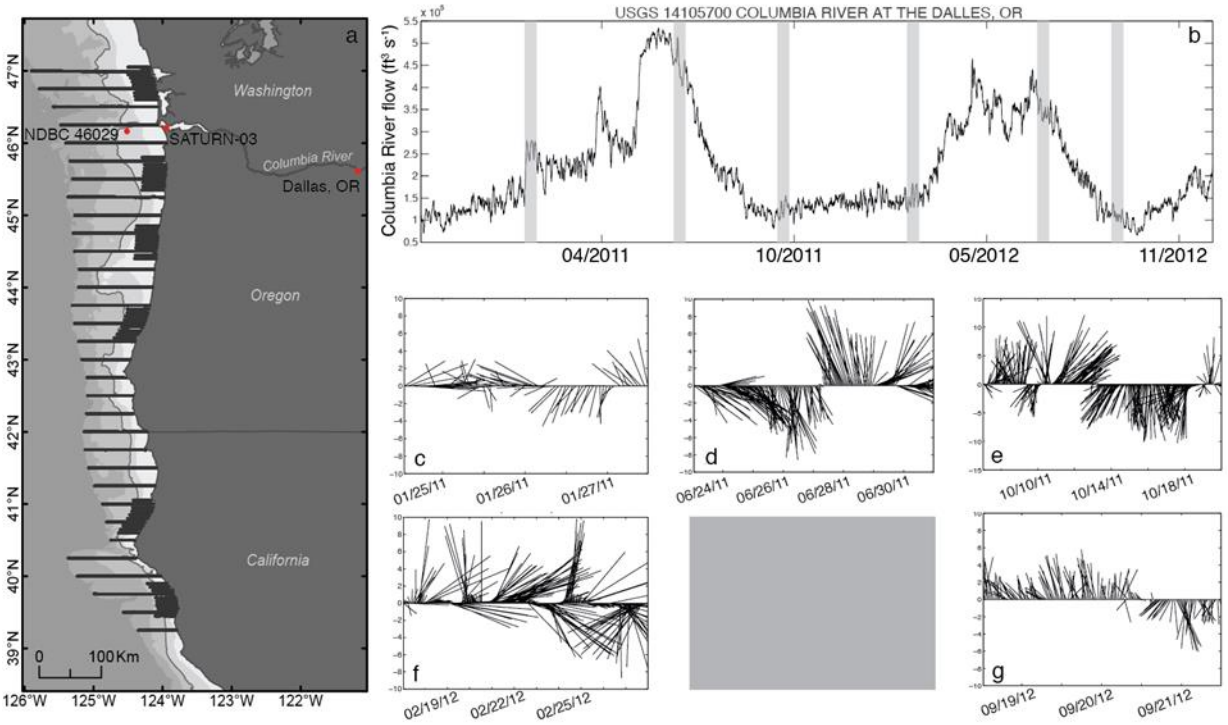

Figure 4. Survey area, Columbia River flow, and winds
A map of the survey area with transect lines is shown in panel a. The 100-m, 1000-m, and 2000-m isobaths are shaded. (b) Columbia River flow rates from The Dalles, Oregon. The gray boxes show the survey dates. Data have been smoothed using a running mean. Winds (c-g) from the National Data Buoy #46029 located at the mouth of the Columbia River plume. No wind data available for the July 2012 survey period (gray panel).

We considered excluding all data collected during cloudy to partially cloudy conditions (above the survey aircraft), but this would have drastically reduced the number of remote sensing observations. Clouds alter both the magnitude and spectral shape of incident light, which consequently affected ${}_{n}L_{w}$. Therefore, we divided spectral ${}_{n}L_{w}$ by the integrated area for the full wavelength range to account for the effect of changing magnitude of incidental light. This normalization was necessary because survey data were collected during both cloudy and cloud-free conditions. Although no correction could be made when the spectral quality of light was altered by clouds, dividing by the integral effectively normalized the spectra to a common scale.

To evaluate coarse-scale, seasonal and inter-annual variability in ocean conditions, we present monthly composite averages of Chla concentrations determined using the National Aeronautics and Space Administration (NASA) Moderate Resolution Imaging Spectroradiometer (MODIS). Additionally, we compared two sub-regions of daily 1-km MODIS Chla values to HR3-derived measurements to evaluate the ability of the HR3 to retrieve meaningful ocean color data from our low-elevation survey aircraft. To do this, we downloaded MODIS L1B data from the LAADS website (https://ladsweb.nascom.nasa.gov/data/) and processed these to L2 data using SeaDAS Version 7.2. To correct MODIS L1B data for atmospheric effects, we used a modified atmospheric correction scheme (aer_opt = 1; relative humidity = 75%; aerosol fraction = 0.01) appropriate for the CCS (Ryan et al., 2009).

2.3 Additional environmental data

For 2011–2012, we compiled USGS stream gage river discharge rates for the Columbia River at The Dalles, Oregon (45.608°N, 121.172°W; http://waterdata.usgs.gov/nwis/inventory/?site_no=1410570; Figure 4). Wind speed and direction data were acquired from the National Data Buoy Center #46029, located near the Columbia River mouth (46.159°N, 124.514°W) (http://www.ndbc.noaa.gov/station_history.php?station=46029; Figure 4), and *in situ* Chla measurements for the Columbia River estuary were made available by the Center for Coastal Margin Observation and Prediction (CMOP) SATURN-03 platform (46.208°N, 123.943°W) (http://www.stccmop.org/datamart/observation_network/fixedstation?id=saturn07; Figure 4).

2.4 K-means cluster analysis

We used k-means cluster analysis (Matlab Student Version 2011a), a feature-based classification technique, to delineate and characterize water masses in the NCCS. Feature-based classification uses the inherent variability in multivariate data to reveal structure, making no *a priori* knowledge necessary (Martin Traykovski and Sosik, 2003; Jain, 2010) and thus, introducing less bias (Palacios et al., 2012). Input variables used in our k-means analysis included SST, log10 transformed Chla, a_{CDOM}, and proxy particle load (i.e, $_nL_w[555]$). All variables were re-scaled from 0–1, to weight them equally for our k-means water mass classifications. The k-means clustering analysis computed clusters based on the squared Euclidean distance from the mean of each cluster. For this analysis, with the exception of January 2011 (regionally-limited data set, k = 3), we set k = 4, following Thomas and Weatherbee (2006), who found four water masses to persist in the CRP region of the CCS. We chose k-means cluster analysis rather than hierarchical, or fuzzy c-means clustering, because k-means is considered more robust for clustering data with lower signal-to-noise ratios (Martin Traykovski and Sosik, 2003; Jain, 2010).

3 Results and discussion

3.1 Aerial survey effort

We conducted replicated surveys off northern California, Oregon, and southern Washington on 14–26 January 2011, 23–30 June 2011, 7–19 October 2011, 17–27 February 2012, 1–5 July 2012, and 19–24 September 2012 (Table 1). Inclement weather occasionally interfered with survey effort. For example, we were not able to complete focal-area surveys during February 2012 within the Nehalem and Grays Harbor target zones, although we were able to complete surveys along several broad lines that overlapped these areas. Also, U.S. Department of the Interior aviation flight restrictions for extended overwater operations constrained our maximum offshore extent to 50 NM during February, July, and September 2012 surveys. This restriction only affected survey coverage of the far offshore slope waters (>200-m depth) off northern Oregon and southern Washington, where the continental shelf broadens. We completed a total 26,752 km of standardized survey effort (not including coastal and offshore deadhead segments between transect lines; Table 1). Effort allocated according to bathymetric domain (i.e., depth strata) was approximately proportional to areas occupied by the bathymetric domains of the shelf-slope region, with additional effort targeting regions of the continental shelf (mostly <200-m depth) within the focal areas. Effort was similar among seasons (winter, summer, and autumn) and between years. With respect to depth strata, 47% (12,646 km) covered the slope domain (200–2000-m depth), 33% (8887 km) covered the inner-shelf (0–100-m depth), and 20% (5219 km) covered the outer-shelf (Table 1).

Table 1. Summary of low-elevation aerial survey effort (linear km surveyed) during PaCSEA surveys off northern California, Oregon, and southern Washington.

Year	Month	Survey Dates	Depth Stratum			All Depths
			0 –100 m	100–200 m	200–2000 m	
2011	January	January 14–26	1,780	991	2,285	5,056
	June	June 23–30	1,572	874	2,382	4,828
	October	October 7–19	1,487	893	2,277	4,657
2012	February	February 17–27	1,114	752	1,626	3,492
	July	July 1–5	1,451	846	2,055	4,352
	September	September 19–24	1,483	863	2,021	4,367
All Surveys			8,887	5,219	12,646	26,752

3.2 Remote sensing

Winter surveys revealed the least amount of regional variability in SST (Figure 5). In January 2011, coolest temperatures (5–6°C) were confined to the relatively small region nearshore off the Columbia River, Willapa Bay, and Grays Harbor. The region of coolest water was more extensive in February 2012 and reached beyond the shelf into the slope domain (i.e., >200 m depth) and farther south off northern Oregon. The onset of regional upwelling during spring and summer caused increased heterogeneity in the SST of the PaCSEA region. In June 2011, relatively warmer waters (16–18°C) emanating from the Columbia River appeared to be transported toward the southwest and extended at least to the slope domain (>200 m depth) off central Oregon (Figure 5). Closer to shore, cold waters (11–12°C) occurred off south-central Oregon north of Cape Blanco (Figure 5). There was no distinct CRP in July 2012, and the region of upwelling did not extend north of Cape Blanco (Figure 5). Fall surveys during October 2011 and September 2012 revealed SST distributions associated with low river flow and regional, autumn relaxation events, though there was a signature of sustained coastal upwelling during September 2012 off central-southern Oregon (Figure 5). October 2011 surveys revealed incursions of warmer waters north of Cape Blanco, Oregon, and south of Cape Mendocino, with small pockets of cooler waters near Cape Mendocino. In September 2012, the signal from warmer offshore waters was evident over the slope domain north of Cape Blanco outside a thin band of cooler waters adjacent to the coast (Figure 5).

Capturing small-scale variability in Chla derived from remote sensing satellite data is particularly challenging in regions like PaCSEA that have persistent seasonal cloud cover. Monthly 4-km MODIS composite Chla images during January 2011 and February 2012 revealed the least amount of variability and the least concentrations overall in regional surface Chla throughout the NCCS (Figure 6). The airborne HR3 measurements show the opposite pattern, with greater median Chla concentrations (Figure 7, Table 3). This discrepancy likely results from small-scale (daily, ≤1-km) variability missed when data are averaged over greater spatiotemporal scales (e.g., MODIS composite imagery). Additionally, the relatively short snapshots acquired from *in situ* airborne measurements are not necessarily representative of average seasonal conditions, and therefore monthly MODIS composites are useful for providing seasonal context.

Although summer Chla concentrations were greatest over the inner-shelf with some discrete hotspot regions, satellite and airborne data demonstrated important differences in distribution patterns. During June 2011, the greatest satellite-based Chla concentrations were associated with the Cape Blanco/Heceta Bank region off Oregon and the Cape Mendocino region off northern California (Figure 6). *In situ* HR3 data revealed comparable Chla data to satellite Chla concentrations in the Cape Blanco/Heceta Bank

region bur lesser magnitude Chla off the Columbia River mouth (Figures 6, 7). Satellite Chla during July 2012 displayed a similar pattern as June 2011, but areas of relatively greater Chla concentrations extended farther north through central Oregon, but not south of Cape Mendocino (Figure 6). The SW offshore bulge of the CRP observed during June 2011 is not as extensive during July 2012 and slightly greater Chla concentrations were instead elevated to the north and south of the Columbia River mouth along the inner shelf (Figures 6, 7).

Patterns in autumn Chla distributions were generally consistent between MODIS and HR3 platforms (Figures 6, 7). October 2011 satellite and HR3 data revealed greatest surface Chla concentrations near the shelf break off Grays Harbor, Washington, near the Columbia River Plume, near the California/Oregon border, and south of Cape Mendocino, California (Figures 6, 7). During September 2012, greatest Chla concentrations were observed off south-central Oregon near Heceta Bank and over the inner-shelf from Cape Blanco, Oregon south to Cape Mendocino, California (Figures 6, 7).

We observed important differences between satellite and airborne Chla measurements in the winter and summer surveys, which highlights the benefits of collecting ocean color data from low-flying aircraft. The ability to survey during periods when cloud cover would obscure satellite remote sensing is particularly critical in regions of persistent cloud cover. Furthermore, airborne data collected during *in situ* sampling should be more closely associated with simultaneous observations of marine birds and mammals, thereby providing an alternative to more limited and spatiotemporally mismatched composite satellite data.

Table 2. Airborne flights with concurrent environmental data. USGS stream gage river discharge rates from The Dalles, Oregon are in units of cubic feet per second. Wind speed and direction are observations from the National Data Buoy #46029, located near the Columbia River mouth. Wind speed (m s^{-1}) is averaged over an eight-min period and wind direction is the direction the wind is coming from in degrees clockwise from true north. Median values are in parentheses.

Flight Period	Latitude Range	Longitude Range	% Usable HR3 Data	River Flow	Wind Speed	Wind Direction
25–27 January 2011	45.496N–47.069N	125.327W–123.956W	99	$1.86X10^5$–$2.67X10^5$	0–10.6 (3.9)	4–359 (176)
23–30 June 2011	39.250N–47.050N	125.899W–123.791W	96	$4.16X10^5$–$4.79X10^5$	0.2–10.5 (5.4)	1–358 (277)
7–19 October 2011	39.250N–47.051N	125.889W–123.780W	99	$1.10X10^5$–$1.44X10^5$	0.1–12.6 (6.2)	1–360 (184)
18–27 February 2012	39.249N–47.006N	125.362W–123.794W	94	$1.30X10^5$–$1.63X10^5$	0.1–14.1 (6.5)	1–358 (201)
1–5 July 2012	39.247N–47.053N	125.416W–123.783W	96	$3.63X10^5$–$3.97X10^5$	1.4–10.1 (6.4)	1–360 (334)
19–24 September 2012	39.250N–47.052N	125.421W–123.784W	99	$1.05X10^5$–$1.24X10^5$	0–11.3 (5.2)	1–359 (172)

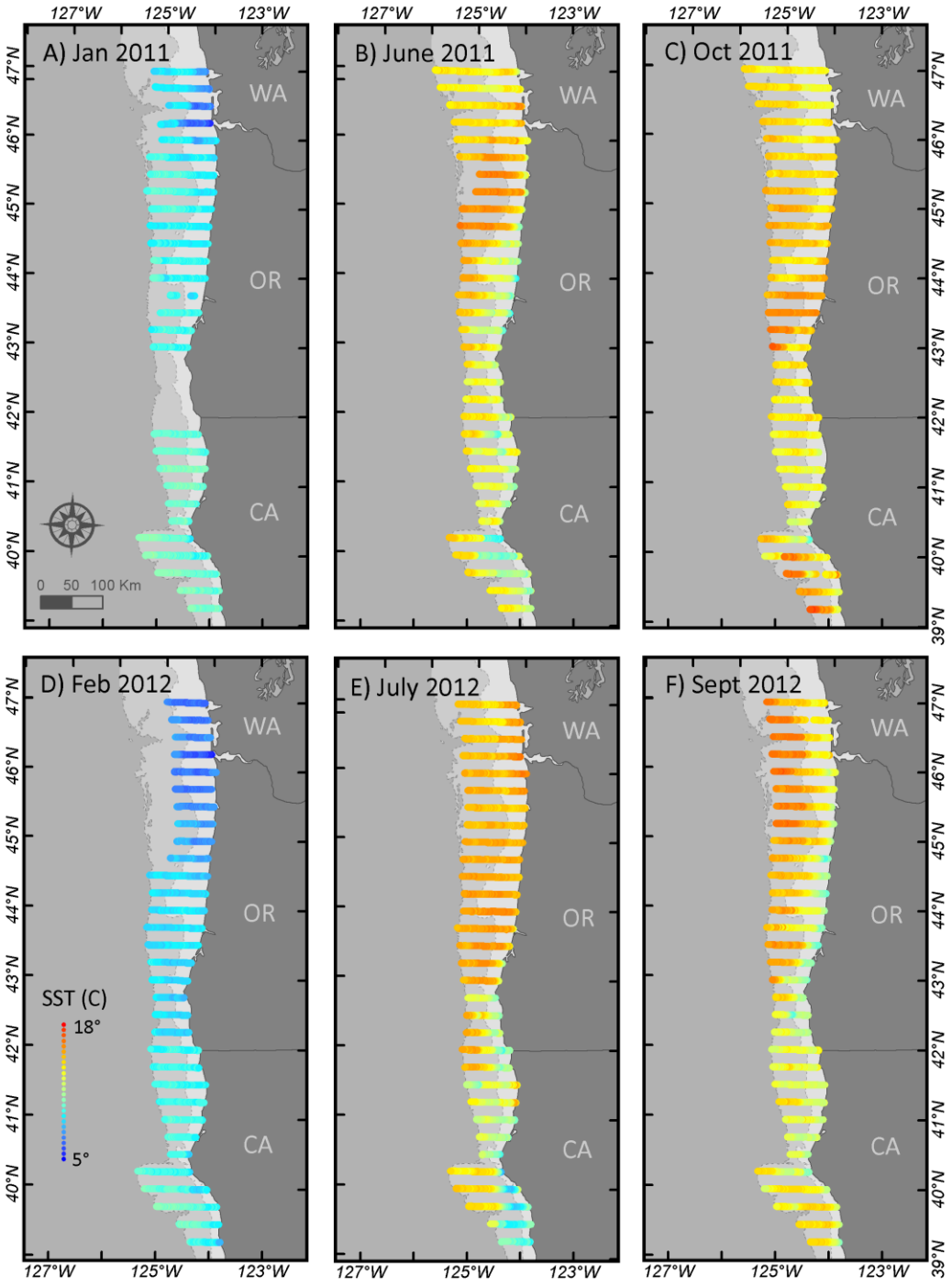

Figure 5. Sea surface temperature
Sea surface temperature (SST, °C) from aircraft-mounted infrared pyrometer collected along replicated, broad transect surveys during winter (A, D), summer (B, E), and fall (C, F). Gaps in (A) off southern Oregon represent missing temperature data only and do not reflect patterns in continuous survey trackline effort.

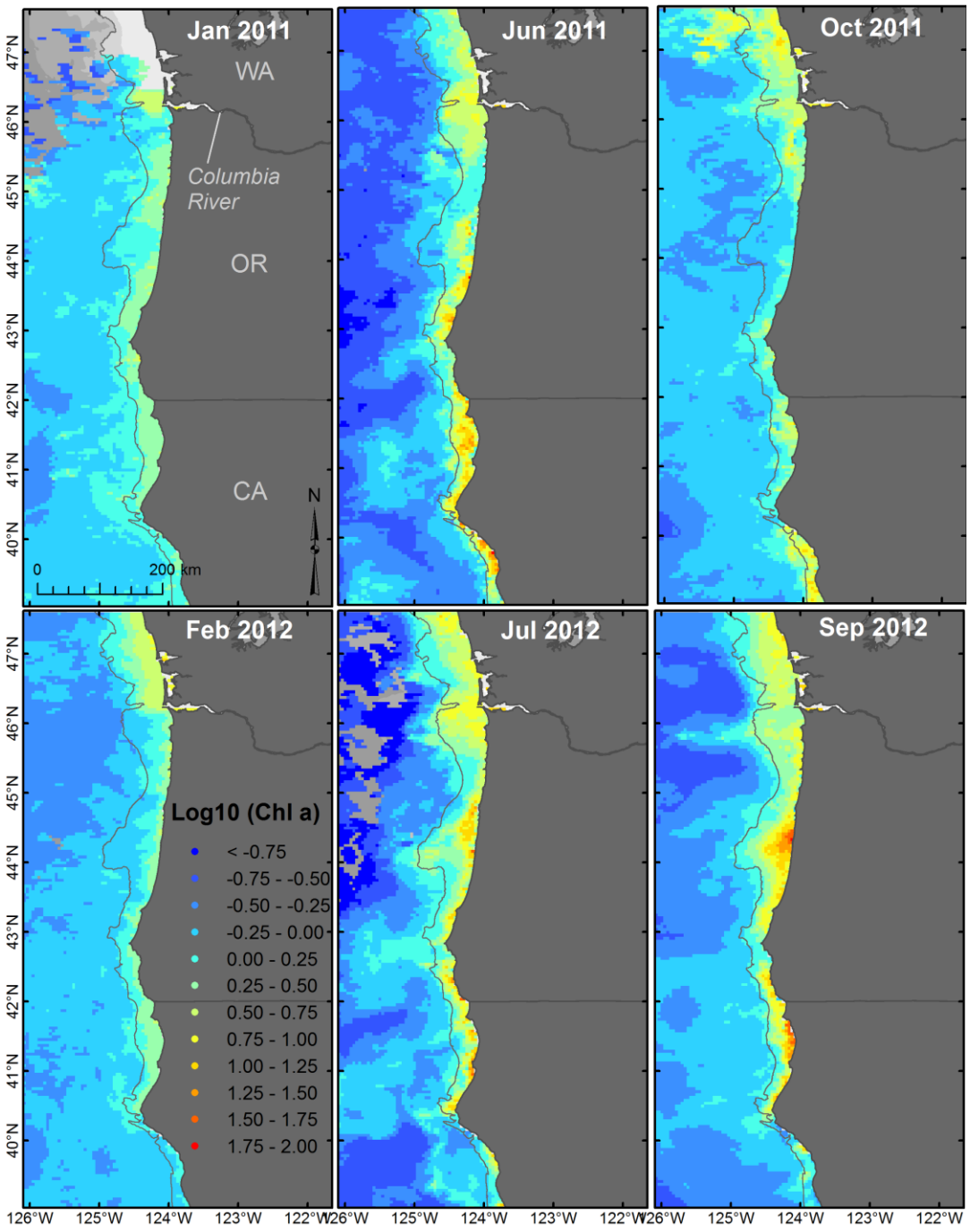

Figure 6. Monthly MODIS satellite imagery
Monthly composite Moderate Resolution Imaging Spectroradiometer (MODIS) satellite imagery (NASA Aqua MODIS Chlorophyll *a,* log10 mg Chla m^{-3}; 4-km pixel resolution) for the northern California Current Region during each of the six PaCSEA survey windows. NASA's OceanColor Web distributes chlorophyll *a* concentration data from NASA's Aqua Spacecraft. Available via https://oceancolor.gsfc.nasa.gov/ (accessed 28 August 2019).

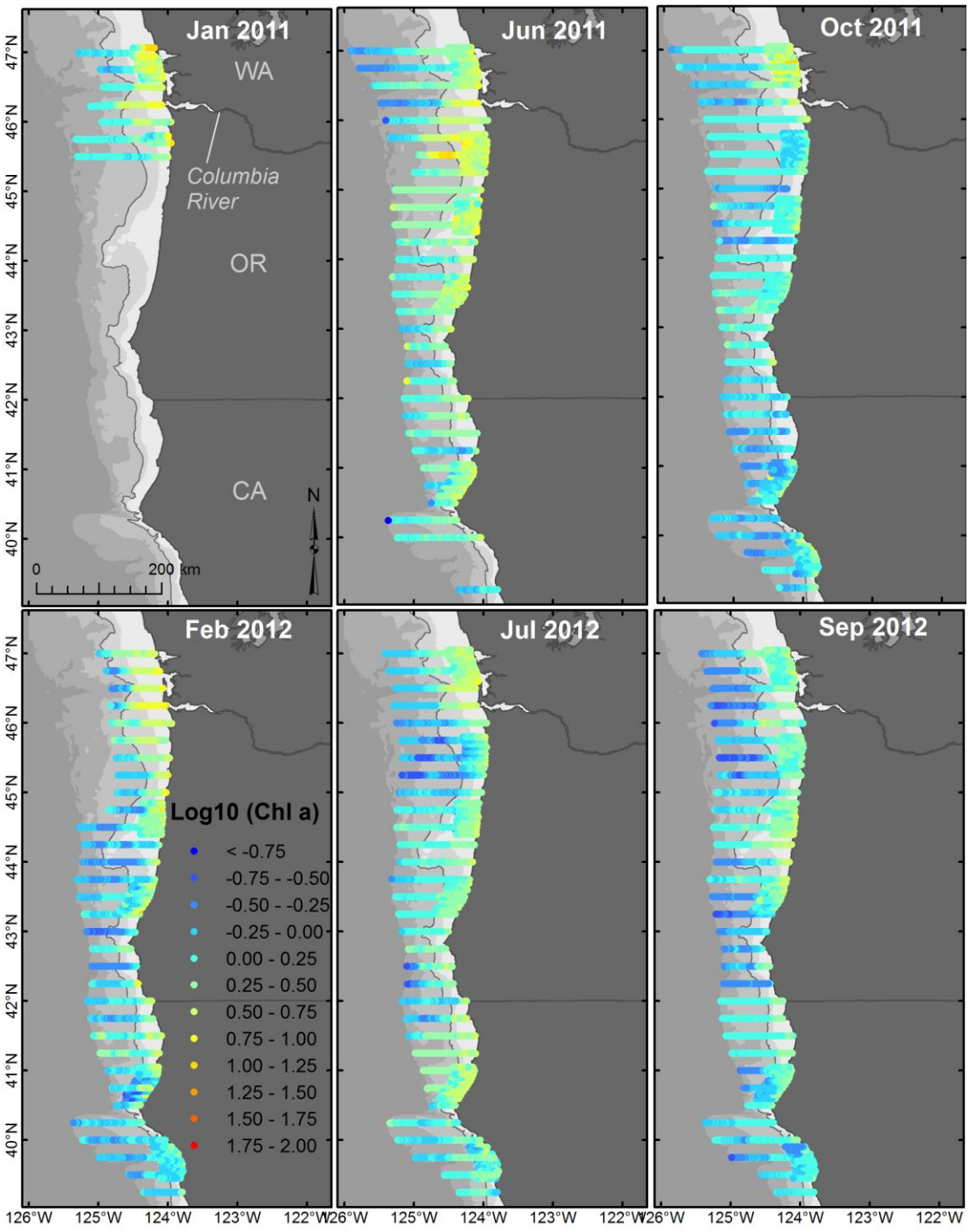

Figure 7. Chlorophyll *a* concentrations derived from HydroRad3 ocean color
Chlorophyll *a* concentrations (log10[mg Chla m^{-3}]) derived from airborne HR3 data shown on the same scale for all surveys, and with the same color-ramp as Figure 6.

3.2.1 Airborne HR3 matchups with MODIS satellite data

The best two MODIS to HR3 matchups are shown in Figure 8. Only subsets of the MODIS images were cloud-free and thus available for matchup to HR3 data. Using the modified atmospheric correction scheme, the distributions of Chla values between sensors were similar (Figure 8c, h) and the structure and gradients of Chla in the HR3 data were realistic and comparable with MODIS images (Figure 8d, e, i, j).

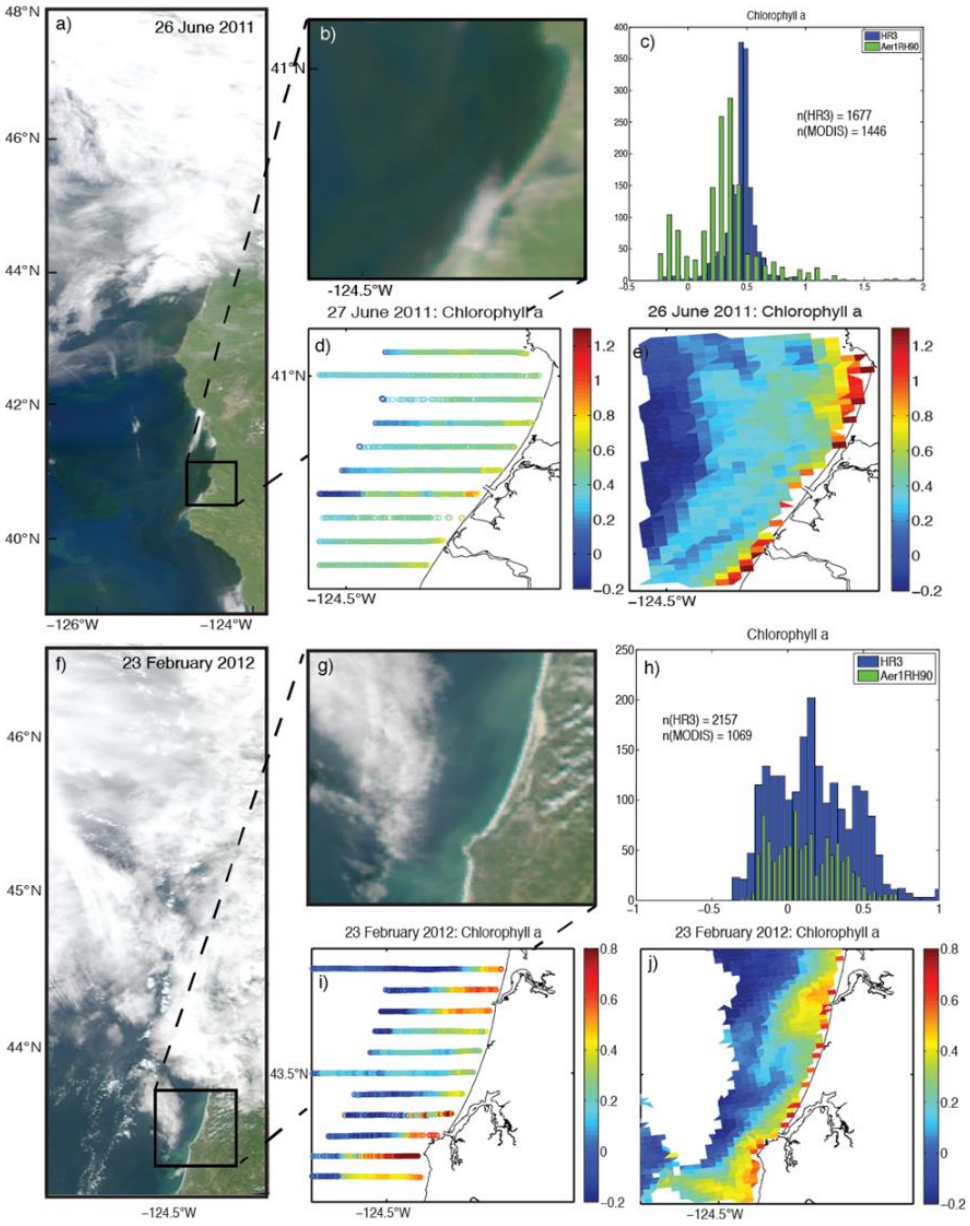

Figure 8. MODIS satellite remote-sensing matchups with HydroRad3
MODIS satellite remote-sensing matchups to HydroRad3 *in situ* chlorophyll *a* data. Panels a-e show data from 26–27 June 2011 and panels f–j show data from 23 February 2012 included are zoomed visible images (b, g), histograms showing frequency (y-axes) distributions (c, h), and survey and MODIS chlorophyll *a* concentrations (log10 [mg m^{-3}]) (d, e) and (I, j), respectively.

3.3 K-means clustering analysis

3.3.1 Winter surveys

The winter 2011 survey period lasted from 14–26 January, but HR3 ocean color data were only available for the northern section of the survey region, including the CRP sampled during 25–27 January. Columbia River discharge during the survey period was moderate and relatively constant, and wind stress was relatively weak (Table 2, Figure 4). K-means clustering identified a bi-directional *CRP* water mass (hereafter, italics are used to identify water mass descriptors) that bulged at the Columbia River mouth (Figure 9). *CRP* was the coldest water mass (7.8°C median value; Table 3) and had the greatest median Chla (5.3 mg m^{-3}), a_{CDOM} (0.6 Au), and proxy particle load (0.7) (Table 3). *Offshore* water was the warmest (9.4°C median value; Table 3) and had the lowest median Chla (1.3 mg m^{-3}), a_{CDOM} (0.4 Au) and proxy particle load (0.2) (Table 3, Figure 9). *Aged CRP* water had intermediate values for all variables, and clustering analysis likely identified waters where *CRP* water mixed with *offshore* water (SST = 8.6°C, Chla = 2.6 mg m^{-3}, a_{CDOM} = 0.5 Au, proxy particle load = 0.5) (Table 3). The boundary between *aged CRP* and *offshore* waters was located over the continental shelf except for the transect intersecting the Columbia River mouth, where *CRP* water extended beyond the shelf break (>200-m depth; Figure 9).

The 2012 winter survey period (18–27 February) was characterized by moderate river flow (less flow than during the 2011 winter survey period) and variable, strong winds (Table 2, Figure 4). K-means clustering again identified a bi-directional *CRP* water mass (44.5°N to 47°N, the northern extent of survey area). Similar to the 2011 winter survey, *CRP* water was the coldest water mass (7.1°C) and had the greatest median Chla (3.9 mg m^{-3}) (Table 3, Figure 9). More extensive regional coverage and best clustering with k = 4 allowed identification of more variable watermasses during winter 2012. *Aged CRP* identified during 2011 were better described by *nearshore* and *intermediate* waters, with the boundary between the two types located over the outer continental shelf between the 100-m and 200-m isobaths. Kudela et al. (2006) found the continental shelf was a natural boundary between optically-distinct shelf and open ocean waters, consistent with the frontal region identified here using k-means clustering. The *intermediate* water mass had similar SST compared with *nearshore* and *offshore* waters, and extended over Heceta Bank off Oregon. The SST of *nearshore* water (8.9°C) was similar to *intermediate* (9.4°C) and *offshore* (9.1°C) waters and had greater Chla (2.4 mg m^{-3}), a_{CDOM} (0.6 Au), and proxy particle load (0.7) compared with *intermediate* and *offshore* waters (Table 3, Figure 9). This pattern indicated that upwelling did not appear to be the primary mechanism supplying nutrients to this water mass, consistent with expectations during no/low upwelling during winter (Banas et al., 2009). We suggest stream/river discharge and interaction with the bottom through enhanced mixing during storm events were the primary sources of nutrient input during this winter survey period.

Table 3. Summary of k-means clustering results. Color ID refers to water mass descriptors presented in Figures 9–11. Percent of pixels (a measure of area), and ranges for sea surface temperature (SST), chlorophyll *a* (Chla; mg Chla m^{-3}), absorption coefficient of colored dissolved organic material (a_{CDOM}) and detritus, and a proxy particle load ($_nL_w$[555]) are shown. a_{CDOM} and proxy particle load values have been rescaled from 0–1.0; median values are in parentheses.

Survey	Water Mass #	Water mass Descriptor	Color ID	% Pixels	SST (°C)	Chla (mg m^{-3})	a_{CDOM} (Au)	Particle load
Jan-2011	1	Offshore	Blue	46	7.3–10.5 (9.4)	0.4–2.3 (1.3)	0.3–0.5 (0.4)	0–0.4 (0.2)
	2	CRP	Green	30	5.3–9.3 (7.8)	2.1–19.8 (5.3)	0.5–0.7 (0.6)	0.5–1.0 (0.7)
	3	Aged CRP	Red	24	6.8–9.8 (8.6)	1.0–5.6 (2.6)	0.4–0.6 (0.5)	0.2–0.7 (0.5)
Jun-2011	1	Aged CRP	Yellow	25	13.0–16.3 (14.6)	1.0–8.3 (2.3)	0.4–0.5 (0.5)	0.3–0.7 (0.3)
	2	CRP	Green	10	10.0–16.7 (15.0)	1.9–18.4 (4.9)	0.5–0.7 (0.6)	0.5–1.0 (0.6)
	3	Offshore	Blue	29	10.4–15.9 (13.8)	0.3–2.5 (1.1)	0.3–0.5 (0.4)	0–0.5 (0.2)
	4	Nearshore	Red	36	7.8–13.4 (11.9)	1.0–10.0 (2.7)	0.4–0.6 (0.5)	0.2–0.9 (0.3)
Oct-2011	1	Warm offshore	Red	37	13.5–16.8 (14.8)	0.6–4.9 (1.5)	0.4–0.5 (0.4)	0.1–0.6 (0.3)
	2	CRP & nearshore	Green	11	11.4–15.7 (13.3)	1.0–19.4 (2.7)	0.4–0.7 (0.5)	0.4–1.0 (0.6)
	3	Offshore	Blue	34	10.5–17.3 (13.8)	0.3–1.5 (0.7)	0.3–0.5 (0.4)	0–0.4 (0.2)
	4	Intermediate	Yellow	18	9.8–14.8 (13.3)	0.7–6.1 (1.4)	0.4–0.5 (0.4)	0.2–0.8 (0.4)
Feb-2012	1	Nearshore	Red	19	6.4–10.3 (8.9)	0.9–6.6 (2.4)	0.5–0.9 (0.6)	0.4–1.0 (0.7)
	2	Offshore	Blue	34	6.9–11.1 (9.1)	0.3–1.6 (0.6)	0.3–0.6 (0.4)	0–0.4 (0.2)
	3	CRP	Green	11	5.3–9.4 (7.1)	1.9–14.4 (3.9)	0.5–0.9 (0.6)	0.5–1.0 (0.8)
	4	Intermediate	Yellow	35	6.7–11.0 (9.4)	0.5–4.1 (1.2)	0.4–0.6 (0.5)	0.2–0.6 (0.4)
Jul-2012	1	Intermediate	Yellow	31	12.7–16.4 (15.2)	0.8–2.5 (1.6)	0.4–0.5 (0.4)	0.3–0.6 (0.4)
	2	CRP & nearshore	Green	21	11.8–16.7 (15.1)	1.3–7.3 (2.7)	0.4–0.6 (0.5)	0.4–0.9 (0.5)
	3	Offshore	Blue	22	11.6–15.8 (14.8)	0.2–1.2 (0.7)	0.3–0.4 (0.4)	0–0.4 (0.2)
	4	Nearshore south	Red	26	7.9–13.2 (11.2)	0.5–7.1 (2.0)	0.4–0.7 (0.5)	0.2–1.0 (0.5)
Sep-2012	1	Intermediate	Yellow	32	10.1–16.5 (13.6)	0.4–2.0 (1.1)	0.3–0.5 (0.4)	0.2–0.5 (0.3)
	2	Nearshore	Red	26	9.2–12.9 (11.6)	0.6–5.8 (1.8)	0.4–0.5 (0.4)	0.3–1.0 (0.5)
	3	Offshore north	Blue	19	11.3–16.9 (15.4)	0.3–1.1 (0.4)	0.3–0.4 (0.4)	0–0.4 (0.2)
	4	CRP	Green	23	12.1–15.9 (13.8)	0.9–6.8 (1.8)	0.4–0.6 (0.5)	0.3–0.9 (0.6)

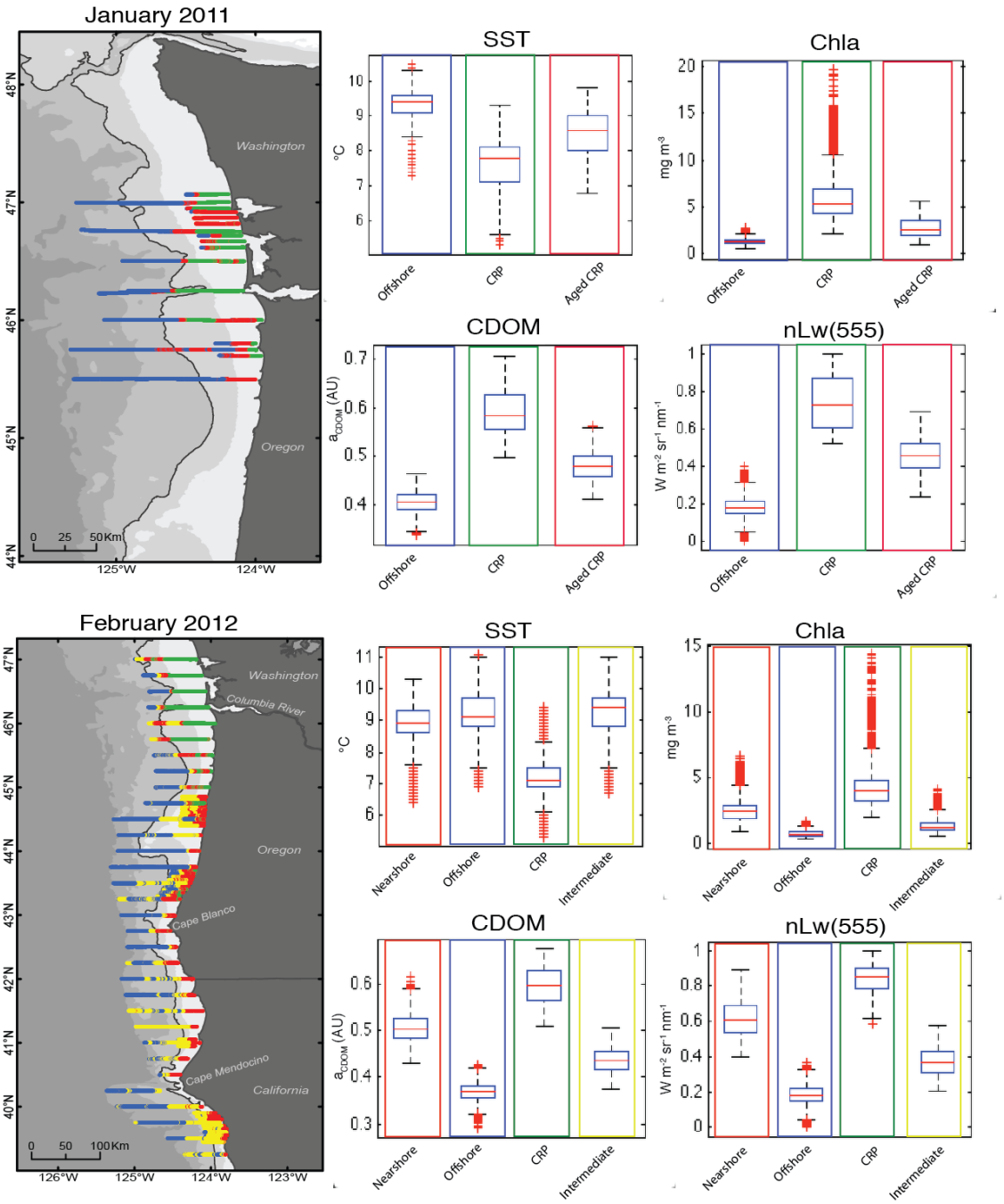

Figure 9. K-means results for winter surveys

Water mass classifications are indicated by color. The box plots on the right show the distribution of sea surface temperature (SST), chlorophyll *a* (Chla), absorption of colored dissolved organic material (a_{CDOM}) and detritus, and proxy particle load ($_{n}L_{w}$[555], scaled 0–1.0) for each water mass. For whisker plots, red horizontal line indicates the the median, and the bottom and top edges of the box indicate the 25th and 75th percentiles, respectively. The whiskers extend to the most extreme data points not considered outliers, and the outliers are plotted individually using the red '+' symbol.

3.3.2 Summer surveys

During summer 2011, we sampled from 23–30 June. River discharge was the greatest recorded throughout any of the survey periods, and the wind was relatively strong, changing direction partway through the survey (Table 2, Figure 4). *CRP* water clustered separately from *aged plume* water, which extended about 200 km southwest from the Columbia River mouth (Figure 10). The SST of the *CRP* water was similar to *aged plume* water (15.0°C versus 14.6°C), but *CRP* water had greater Chla, a_{CDOM}, and proxy particle load (4.9 mg m^{-3}, 0.6 Au, and 0.6 versus 2.3 mg m^{-3}, 0.5 Au, and 0.3, respectively; Table 3, Figure 10). *Offshore* water extended the length of the survey area and had the lowest median Chla, a_{CDOM}, and proxy particle load (1.1 mg m^{-3}, 0.4 Au, and 0.2, respectively). The median SST (13.8°C, Table 3, Figure 10) was intermediate compared with the other water masses identified. *Nearshore* (newly upwelled) water was the coldest (11.9°C) and had similar Chla, a_{CDOM}, and proxy particle load as the *aged plume* (2.7 mg m^{-3}, 0.5 Au, and 0.3, respectively, versus SST = 14.6°C, 2.3 mg m^{-3}, 0.5 Au, and 0.3, respectively; Table 3, Figure 10). The boundary between these two water masses was located at the shelf break or offshore (Figure 10).

During the July 2012 survey period, the boundaries of the *CRP* were less distinct and different from clusters observed in 2011. We identified a unified cluster as *plume/nearshore* water (Figure 10). This water mass formed a bulge at the mouth of the Columbia River and extended northward (Figure 10). Very nearshore water south to Cape Blanco (<100 m depth) also clustered with this water mass. *Intermediate* water bordered the plume and extended south along the coast to Cape Blanco and across the shelf break (Figure 11). South of Cape Blanco, *nearshore south* water was colder (11.2°C) and had greater Chla, a_{CDOM}, and proxy particle load (2.0 mg m^{-3}, 0.5 Au, and 0.5, respectively; Table 3, Figure 10), indicative of strong upwelling at Cape Mendocino and with the presence of a frontal boundary extending offshore. This thermal frontal boundary is well documented (Barth et al., 2000; Huyer et al., 2005; Venegas et al., 2008) and is hypothesized to be a response to differential forcing combined with bathymetry and coastline orientation. *Offshore* water, unlike the two nearshore water masses, extended the entire length of the survey and had the lowest median Chla, a_{CDOM}, and proxy particle load (0.7 mg m^{-3}, 0.4 Au, and 0.2, respectively; Table 3; Figure 10).

CRP Chla concentrations in June 2011 and July 2012 ranged from 1.6–18.4 mg m^{-3} (median = 4.9 mg m^{-3}) and 12.3–16.7 mg m^{-3} (median = 15.2 mg m^{-3}), respectively. Chla at SATURN-03, located inside the Columbia River mouth (Figure 4), in June 2011 ranged from 2.5–8.0 mg m^{-3} and July 2012 ranged from 2.5–6.0 mg m^{-3}. In June 2011, river flow was high and the core plume was relatively small. Although upwelling was occurring (indicated by low coastal SST in the region), the range of plume Chla values overlapped with Chla concentrations measured in the estuary. However, the range of Chla in *aged plume* water was lower than the *CRP* perhaps indicating mixing effects or consumption by grazers. This is consistent with Peterson and Peterson (2008) who observed the greatest zooplankton concentrations in older, aged plume water. Likewise, we might expect to find greater relative abundances of mesotrophic fish and seabirds within *aged plume* water.

Conversely in July 2012, *CRP & nearshore* Chla concentrations were much higher than in the estuary. Relatively homogenous SST values across the continental shelf indicated that weak or no upwelling occurred north of Cape Blanco just prior to or during the July 2012 survey period. Elevated Chla concentrations observed in the CRP may have resulted from a northward flowing plume that blocked southward flow of California Current water, causing this water mass to be retained on the continental shelf, and consequently creating a more stable environment to promote phytoplankton growth. However, these data only provided a snapshot for the cumulative effects of multiple, dynamic ocean processes (i.e., tides, internal waves, upwelling preceding survey period) which also may have contributed to the observed pattern.

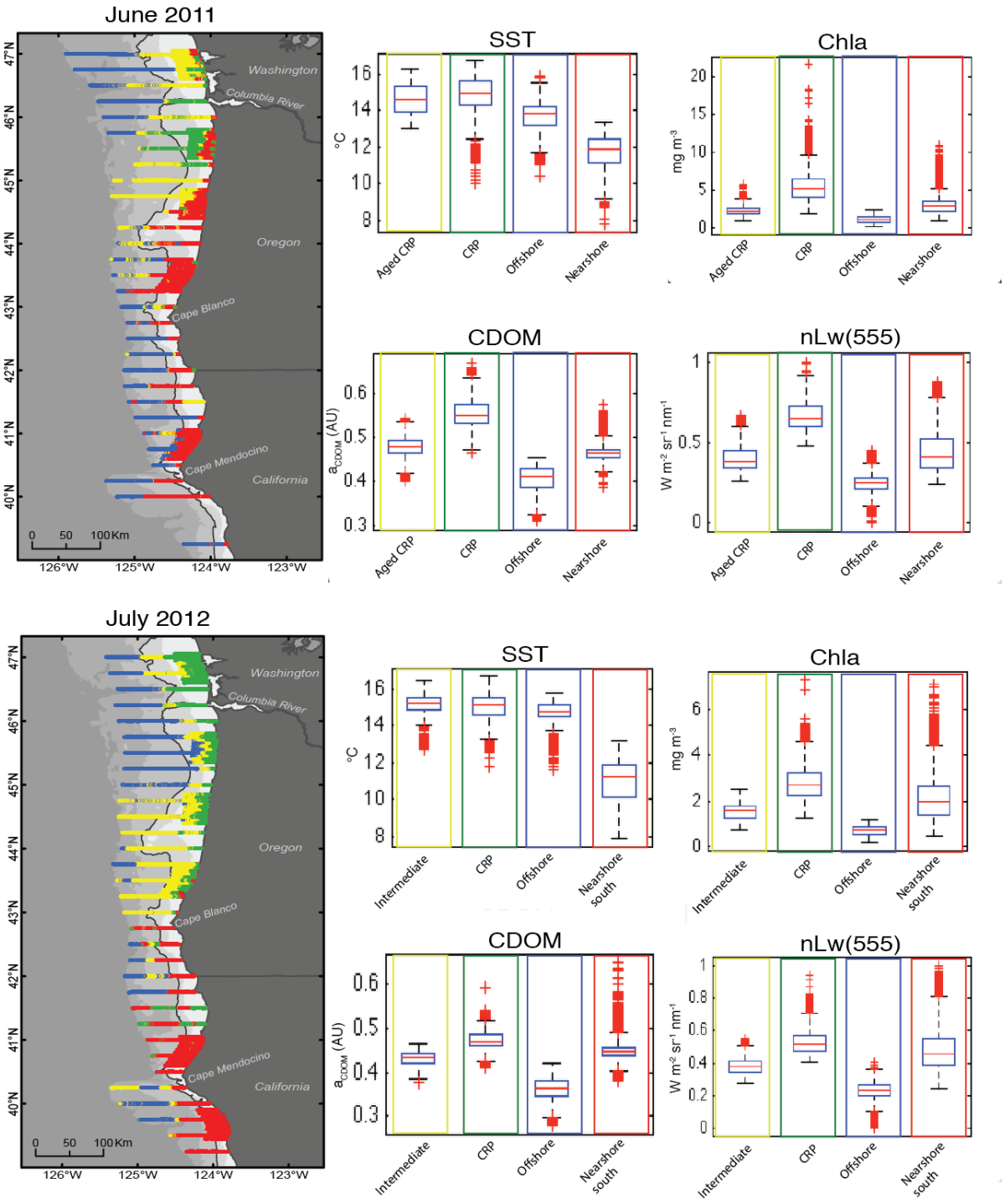

Figure 10. K-means results for summer surveys

Water mass classifications are indicated by color. The box plots on the right show the distribution of sea surface temperature (SST), chlorophyll *a* (Chla), absorption of colored dissolved organic material (a_{CDOM}) and detritus, and proxy particle load ($_{n}L_{w}$[555], scaled 0–1.0) for each water mass. For whisker plots, red horizontal line indicates the the median, and the bottom and top edges of the box indicate the 25th and 75th percentiles, respectively. The whiskers extend to the most extreme data points not considered outliers, and the outliers are plotted individually using the red '+' symbol.

3.3.3 Autumn surveys

The Autumn surveys (7–19 October 2011) occurred during the lowest Columbia River flow rates when wind speeds were among the greatest observed (Figure 4). K-means clustering identified *CRP* water extended offshore and north of the river mouth (Figure 11). Very nearshore water south of the plume and water around Cape Mendocino (*CRP & nearshore* water) had the greatest Chla, a_{CDOM} and proxy particle load, and clustered with *CRP* water (13.3°C, 2.7 mg m^{-3}, 0.5 Au, and 0.6, respectively; Table 3, Figure 11). *Intermediate* water (13.3°C, 1.4 mg m^{-3}, 0.4 m^{-1}, and 0.4), both at the CRP boundary and around Cape Mendocino, likely resulted from mixing of *CRP & nearshore* water with *warm offshore* water (14.8°C, 1.5 mg m^{-3}, 0.4 m^{-1}, and 0.3; Table 3, Figures 5, 11). A second *offshore* water mass extended the full latitudinal range of the survey area, and had the lowest median Chla, a_{CDOM}, and proxy particle load (13.8°C, 0.7 mg m^{-3}, 0.4 Au, and 0.2, respectively; Table 3, Figure 11). We observed high Chla values north of the CRP during October 2011 (<100 m depth; >15 mg m^{-3}). This pattern is similar to July 2012, and also indicates a northward flowing plume retained on the Washington shelf. It is possible that an additional nutrient source was entrained in the plume, allowing accumulation of phytoplankton biomass and greater Chla at the surface.

In contrast to October 2011, during 19–24 September 2012, we sampled during some of the weakest wind speeds observed. The *CRP* was bi-directional and extended southwestward near Heceta Bank. Isolated observations of similar waters occurred very nearshore between Capes Blanco and Mendocino (Figure 11). *CRP* water (13.8°C, 1.8 mg m^{-3}, 0.5 Au, and 0.6) had similar median SST as *intermediate* water (13.6°C, 1.1 mg m^{-3}, 0.4 Au, 0.3), but had greater Chla, a_{CDOM}, and proxy particle load (Table 3, Figure 11). *Nearshore* water extended from south of the Columbia River to south of Cape Mendocino over a large portion of the continental shelf. This was the coldest water mass, with Chla, a_{CDOM}, and proxy particle load similar to the *CRP* (11.6°C, 1.8 mg m^{-3}, 0.4 Au, and 0.5, respectively; Table 3, Figure 11). *Offshore* water was located predominantly north of Cape Blanco, and had the warmest SST with the lowest Chla, CDOM, and proxy particle load (15.4°C, 0.4 mg m^{-3}, 0.4 m^{-1}, and 0.2, respectively; Table 3, Figure 11). The majority of observations were classified as *intermediate*, with SST similar to the CRP, and Chla, a_{CDOM}, and proxy particle load all of intermediate values, between *offshore* and *CRP* water. This water mass was located at the CRP boundary, where it mixed with *offshore* water, and extended throughout the length of the survey area.

During September 2012, weak, southerly, downwelling-favorable winds persisted for most of the survey, then switched to upwelling favorable winds. The plume region was sampled 23–24 September after several days of moderate NW winds (Figure 4g). A bi-directional *CRP* was consistent with alongshore wind stress that switched from southerly to northerly partially through the survey. Nearshore water had slightly greater median Chla (1.80 mg m^{-3}) than CRP water (1.75 mg m^{-3}), resulting from elevated Chla concentrations over Heceta Bank. Lower SSTs were observed nearshore north of Cape Blanco indicating nutrients in this water mass likely were at least in-part, upwelling-derived.

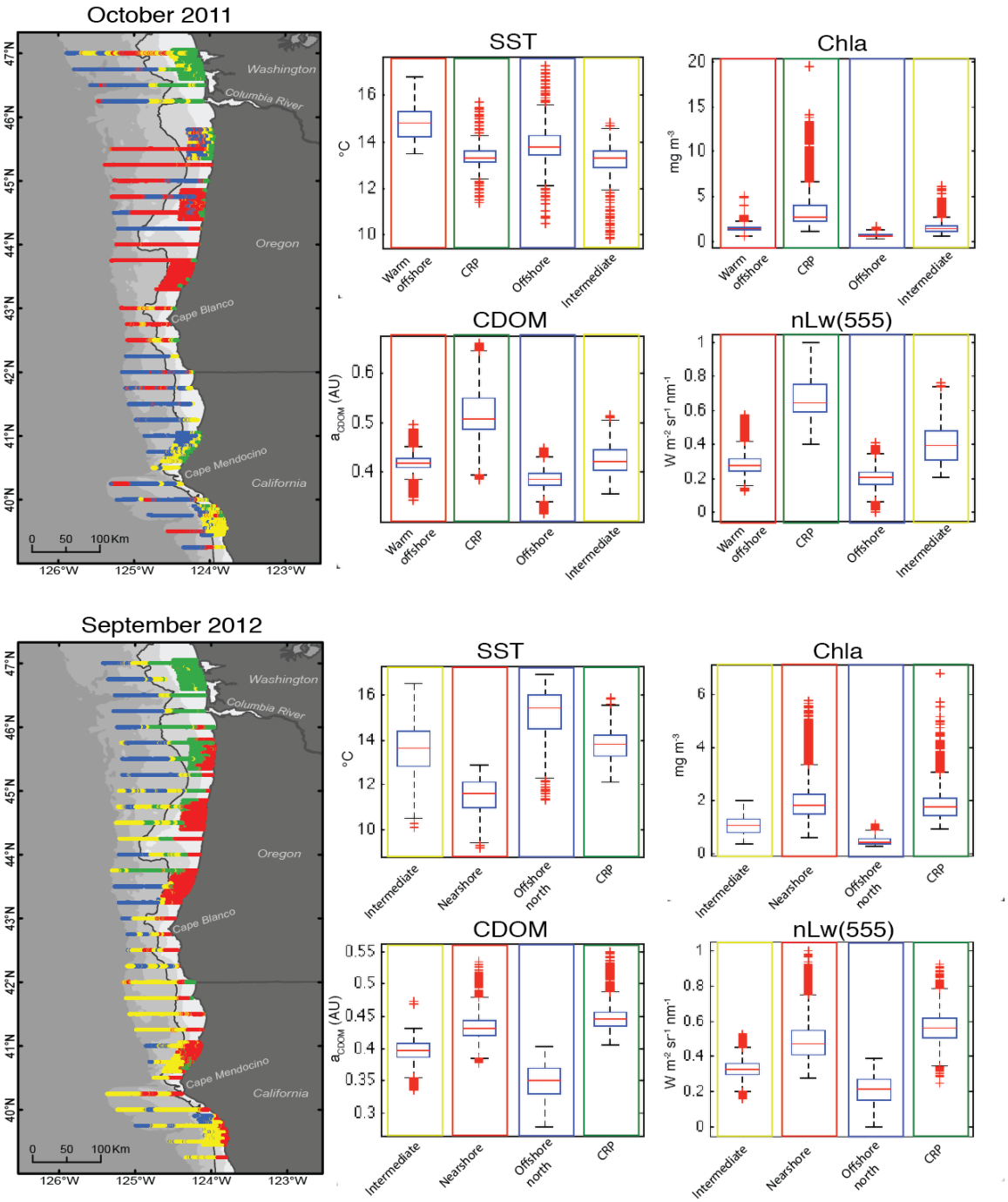

Figure 11. K-means results for autumn surveys

Water mass classifications are indicated by color. The box plots on the right show the distribution of sea surface temperature (SST), chlorophyll *a* (Chla), absorption of colored dissolved organic material (a_{CDOM}) and detritus, and proxy particle load ($_nL_w$[555], scaled 0–1.0) for each water mass. For whisker plots, red horizontal line indicates the the median, and the bottom and top edges of the box indicate the 25th and 75th percentiles, respectively. The whiskers extend to the most extreme data points not considered outliers, and the outliers are plotted individually using the red '+' symbol.

4 Summary and conclusion

This study has demonstrated that airborne ocean color and SST data can be used to characterize water masses associated with the NCCS, including the CRP. We observed variability in water mass boundaries between years and during all seasons, consistent with the expectation of a dynamic, bi-modal CRP (Hickey et al. 2005) and variable forcing driving upwelling. Aircraft-mounted sensors flown at relatively low altitude (60 m) allowed data to be collected when satellite data would have otherwise been unavailable due to cloud cover. For example, of 46 survey days, none had satellite remotely-sensed ocean color data (daily) in >50% of the image.

Aerial surveys have been used extensively to monitor seabird and marine mammal species abundance and distribution patterns at sea (Camphuysen et al., 2004; Buckland et al., 2012). Including an ocean color sensor and aerial pyrometer provides a means to collect *in situ* environmental data useful for investigating some of the underlying mechanisms driving these abundance patterns. Additionally, ocean color data collected from low-flying survey aircraft can be used for long-term monitoring of ocean properties, such as chlorophyll *a* concentrations and other derived properties. For example, during the past two decades, in the Chesapeake Bay, Harding et al., (1992), Harding et al., (1995), and Miller and Harding (2007) used low-flying aircraft to monitor phytoplankton dynamics during cloudy conditions at high spatial resolution. Including ocean color data sensed from low-flying aircraft during future surveys in the Pacific could provide important information on phytoplankton and water mass dynamics over multiple time-scales. Additional study in the future will use these data to assist in the quantification of NCCS seabird community patterns and evaluation of environmental predictors that may prove useful for predicting at-sea abundance.

5 References

Adams J., MacLeod, C., Suryan, R.M., Hyrenbach, D., and Harvey, J.T. (2012) Summer-time use of west coast U.S. National Marine Sanctuaries by migrating sooty shearwaters (*Puffinus griseus*). Biological Conservation 156:105–116.

Adams J., Felis, J., Mason J.W., and Takekawa, J.Y. (2014) Pacific Continental Shelf Environmental Assessment (PaCSEA): aerial seabird and marine mammal surveys off northern California, Oregon, and Washington, 2011–2012. U.S. Dept. of the Interior, BureAu of Ocean Energy Management, Pacific OCS Region, Camarillo, California. OCS Study BOEM 2014-003.

Adams, J., Kelsey, E.C., Felis J.J., and Pereksta, D.M. (2016) Collision and displacement vulnerability among marine birds of the California Current System associated with offshore wind energy infrastructure: U.S. Geological Survey Open-File Report 2016-1154, 116 p., http://dx.doi.org/10.3133/ofr20161154.

Ainley, D.G. Spear, L.B., Tynan, C.T., Barth, J.A., Pierce, S.D., Ford, R.G., and Cowles, T.J. (2005) Physical and biological variables affecting seabird distributions during the upwelling season of the northern California Current. Deep-Sea Research II 52:123–143.

Aguilar-Islas A.M. and Bruland, K.W. (2006) Dissolved manganese and silicic acid in the Columbia River plume: A major source to the California current and coastal waters off Washington and Oregon. Marine Chemistry 101:233–247.

Banas, N.S., Lessard, E.J., Kudela, R.M., MacCready, P., Peterson, T.D., Hickey, B.M., and Frame, E. (2009) Planktonic growth and grazing in the Columbia River plume region: A biophysical model study. Journal of Geophysical Research 114: C00B06, doi:10.1029/2008JC004993.

Barth, J.A., Pierce, S.D., and Smith, R.L. (2000) A separating coastal upwelling jet at Cape Blanco, Oregon and its connection to the California Current System. Deep-Sea Research II 47:783–810.

BOEM (2017) Bureau of Ocean Energy Management. https://www.boem.gov/Renewable-Energy/ (Accessed 9 March 2017).

Bonnell, M.L., C.E. Bowlby, and G.A. Green (1992) Chapter 2: Pinniped Distribution and Abundance off Oregon and Washington, 1989–1990. *In*: J.J. Brueggeman (Ed.) Oregon and Washington Marine Mammal and Seabirds Surveys. Final Report, OCS Study MMS 91-0093, Pacific OCS Region, Minerals Management Service, U.S. Department of the Interior, Los Angeles, California.

Briggs, K.T., Breck Tyler, W.M., Lewis, D.B., and Carlson, D.R. (1987) Bird Communities at Sea Off California 1975 to 1983. Studies in Avian Biology No. 11. The Cooper Ornithological Society. 74 p.

Briggs, K.T., Varoujean, D.H., Williams, W.W., Ford, R.G., Bonnel, M.L., and Casey, J.L. (1992) Chapter 3: Seabirds of the Oregon and Washington OCS, 1989–1990. *In*: J.J. Brueggeman (Ed.) Oregon and Washington Marine Mammal and Seabirds Surveys. Final Report, OCS Study MMS 91-0093, Pacific OCS Region, Minerals Management Service, U.S. Department of the Interior, Los Angeles, California.

Bruland, K.W., Lohan, M.C., Aguilar-Islas, A.M., Smith, G.J. Sohst, B., and Baptista, A. (2008) Factors influencing the chemistry of the near-field Columbia River plume: Nitrate silicic acid, dissolved Fe, and dissolved Mn. Journal of Geophysical Research 113, C00B02, doi:10.1029/2007JC004702.

Buckland, S.T., Burt, M.L., Rexstad, E.A., Mellor, M., Williams, A.E., and Woodward, R. (2012). Aerial surveys of seabirds: the advent of digital methods. Journal of Applied Ecology, 49(4), 960–967.

Camphuysen, C.J., Fox, A.D., Leopold, M.F., and Petersen, I.K. (2004). Towards Standardized Seabirds at Sea Census Techniques in Connection with Environmental Impact Assessments for Offshore Wind Farms in the UK: a comparison of ship and aerial sampling methods for marine birds and their applicability to offshore wind farm assessments.

Devred, E., Sathyendranath, S., and Platt, T. (2007) Delineation of ecological provinces using ocean colour radiometry. Marine Ecology Progress Series 364:1–13.

Doxaran D., Ehn, J., Matsuoka, A., Hooker, S., and Babin, M. (2012) Optical characterization of suspended particles in the Mackenzie River plume (Canadian Arctic Ocean) and implication for ocean colour remote sensing. Biogeosciences 9:3213–3229.

Gordon, H.R. and Voss, K.J. (1999) MODIS Normalized Water-leaving Radiance Algorithm Theoretical Basis Document V4. Department of Physics, University of Miami, NAS5-31363.

Green, G.A., Brueggeman, J.J., Grotefendt, R.A., and Bowlby, C.E. (1992) Chapter 1: Cetacean Distribution and Abundance off Oregon and Washington, 1989–1990. *In*: J.J. Brueggeman (Ed.) Oregon and Washington Marine Mammal and Seabirds Surveys. Final Report, OCS Study MMS 91-0093, Pacific OCS Region, Minerals Management Service, U.S. Department of the Interior, Los Angeles, California.

Harding L.W., Jr., Itsweire E.C., and Esaias, W.E. (1992) Determination of phytoplankton chlorophyll concentrations in the Chesapeake Bay with aircraft remote sensing. Remote Sensing if the Environment 40: 79–100.

Harding, L.W., Jr., Itsweire E.C., and Esaias, W.E. (1995) Algorithm development for recovering chlorophyll concentrations in the Chesapeake Bay using aircraft remote sensing 1989–91. Photogramm. Eng. Rem. Sens., 61: 177–185.

Hickey, B.M., Pietrafesa, L.J., Jay, D.A., and Boicourt, W.C. (1998) The Columbia River Plume Study: Subtiday variability in the velocity and salinity fields. Journal of Geophysical Research 103:10339–10368.

Hickey, B.M., and Banas, N.S. (2008) Why is the Northern End of the California Current System so Productive? Oceanography 21(4):90–107.

Hickey, B.M. and Banas, N.S. (2003) Oceanography of the U.S. Pacific Northwest Coastal Ocean and Estuaries with Application to Coastal Ecology. Estuaries 26:1010–1031.

Hickey, B. Geier, S., Kachel, N., and MacFayden, A. (2005) A bi-directional river plume: The Columbia in summer. Continental Shelf Research 25:1631–1656.

Hickey, B., MacFayden, A., Cochlan, W., Kudela, R., Bruland, K., and Trick, C. (2006) Evolution of chemical, biological, and physical water properties in the northern California Current in 2005: Remote or local wind forcing? Geophysical Research Letters 33, L22S02, doi:10.1029/2006GL026782.

Huyer, A., (1983) Coastal upwelling in the California Current system. Progress in oceanography, 12(3), pp.259–284.

Huyer, A., Fleischbein, J.H., Keister, J., Kosro, P.M., Perlin, N., Smith, R.L., and Wheeler, P.A. (2005) Two coastal upwelling domains in the northern California Current system. Journal of Marine Research 63:901–929.

Jain, A.K. (2010) Data clustering: 50 years beyond K-means. Pattern Recognition Letters 31:651–666.

Kahru, M. and Mitchell, B.G. (2001) Seasonal and nonseasonal variability of satellite- derived chlorophyll and colored dissolved organic matter concentration in the California Current. Journal of Geophysical Research 106(2):2517–2529.

Kahru, M., Kudela, R.M., Manzano-Sarabia, M., and Mitchell, B.G. (2012) Trends in the surface chlorophyll of the California Current: Merging data from multiple ocean color satellites. Deep-Sea Research II 77-80:89–98.

Kelsey, E.C., Felis, J.J., Czapanskiy, M., Pereksta, D.M., and Adams, J. (2018). Collision and displacement vulnerability to offshore wind energy infrastructure among marine birds of the Pacific Outer Continental Shelf. Journal of environmental management, *227*, 229–247.

Kudela, R.M., Garfield, N., and Bruland, K.W. (2006) Optical signatures and biogeochemistry from intense upwelling and relaxation in coastal California. Deep- Sea Research II 53:2999-3022.

Kudela, R.M. and Peterson, T.D. (2009) Influence of a buoyant river plume on phytoplankton nutrient dynamics: What controls standing stocks and productivity? Journal of Geophysical Research 114, C00B11, doi:10.1029/2008JC004913.

Kudela, R.M., Horner_devine, A.R., Banas, N.S., Hickey, B.M., Pterson, T.D., McCabe, R.M., Lessard, E.J., Frame, E., Bruland, K.W., Jay, D.A., Peterson, J.O., Peterson, W.T., Kosro, P.M., Palacios, S.L., Lohan, M.C., and Dever, E.P. (2010) Multiple trophic levels fueled by recirculation in the Columbia River plume. Geophysical Research Letters 37, L18607, doi:10.1029.2010GL044342.

Longhurst, A., Sathyendranath, S., Platt, T., and Caverhill, C. (1995) An estimate of global primary production in the ocean from satellite radiometer data. Journal of Plankton Research 17(6):1245–1271.

Louzao, M., Delord, K., García, D., Boué, A., and Weimerskirch, H. (2012) Protecting Persistent Dynamic Oceanographic Features: Transboundary Conservation Efforts Are Needed for the Critically Endangered Balearic Shearwater. PLoS ONE 7(5): e35728. doi:10.1371/journal.pone.0035728

Martin Traykovski, L.V. and Sosik, H.M. (2003) Feature-based classification of optical water types in the Northwest Atlantic based on ocean color data. Journal of Geophysical Research 108, C5, 3150, doi:10.1029/2001JC001172.

Mason, J.W., McChesney, G.J., McIver, W.R., Carter, H.R., Takekawa, J.Y., Golightly, R.T., Ackerman, J.T., Orthmeyer, D.L., Perry, W.M., Yee, J.L., Pierson, M.O., and McCrary, M.D. (2007) At-sea distribution and abundance of seabirds off southern California: a 20-year comparison. Studies in Avian Biology, No. 33. 95 p.

Menza, C., J. Leirness, T. White, A. Winship, B. Kinlan, L. Kracker, J. E. Zamon, L. Ballance, E. Becker, K. Forney, J. Barlow, J. Adams, D. Pereksta, S. Pearson, J. Pierce, S. Jeffries, J. Laake, J. Calambokidis, A. Douglas, B. Hanson, S. Benson, and L. Antrim (2016) Predicted Distribution Maps of Seabirds, Pinnipeds, and Cetaceans off the Pacific Coast of Washington. NOAA Technical Memorandum NOS NCCOS 210. Silver Spring, MD. 96 p. doi: 10.7289/V5NV9G7Z

Miller, A.J., McWilliams, J.C., Schneider, N., Allen, J.S., Barth, J.A., Beardsley, R.C., Chavez, F.P., Chereskin, T.K., Edwards, C.A., Haney, R.L., Kelly, K.A., Kindle, J.C., Ly, L.N., Moisan, J.R., Noble, M.A., Niiler, P.P., Oey, L.Y., Schwing, F.B Shearman, R.K., and Swenson, M.S. (1999) Observing and Modeling the California Current System. EOS 80(45):533–548.

Miller, W. and Harding Jr, L.W. (2007) Climate forcing of the spring bloom in Chesapeake Bay. Marine Ecology Progress Series, 331:11–22.

Mobley, C.D. (1999) Estimation of the remote-sensing reflectance from above-surface measurements. Applied Optics 38(36):7442–7455.

Mueller, J. L., C. Pietras, S. B. Hooker, R. W. Austin, M. Miller, K. D. Knobelspiesse, R. Frouin, B. Holben, and K. Voss (2003), Ocean optics protocols for satellite ocean color sensor validation, Revision 4, Volume 2: Instrument specifications, characterization, and calibration, in NASA Tech. Memo. 2003 – 211621/Rev4, vol. II, edited by J. L. Mueller, G. S. Fargion, and C. R. McClain, 56 pp., NASA GSFC, Greenbelt, Md.

Nur, N., J. Jahncke, M.P. Herzog, J. Howar, K.D. Hyrenbach, J.E. Zamon, D.G. Ainley, J.A. Wiens, K. Morgan, L.T. Ballance, and D. Stralberg (2011) Where the wild things are: predicting hotspots of seabird aggregations in the California Current System. Ecological Applications 21:2241–2257.

Otero, M.P. and Siegel, D.A. (2004) Spatial and temporal characteristics of sediment plumes and phytoplankton blooms in the Santa Barbara Channel. Deep-Sea Research II 51:1129–1149.

Palacios, S.L., Peterson, T.D., and Kudela, R.M. (2012) Optical characterization of water masses within the Columbia River plume. Journal of Geophysical Research 117, C11020, doi:10.1029/2012JC008005.

Peterson, J.O., and Peterson, W.T. (2008). Influence of the Columbia River plume (USA) on the vertical and horizontal distribution of mesozooplankton over the Washington and Oregon shelf. ICES Journal of Marine Science 65(3):477–483.

Ryan, J.P., Fischer, A.M., Kudela, R.M., Gower, J.F., King, S.A., Marin III, R., & Chavez, F.P. (2009). Influences of upwelling and downwelling winds on red tide bloom dynamics in Monterey Bay, California. *Continental Shelf Research*, *29*(5-6), 785–795.

Suryan, R.M., E.M. Phillips, K.J. So, J.E. Zamon, R.W. Lowe, and S.W. Stephensen (2012) Marine bird colony and at-sea distributions along the Oregon coast: Implications for marine spatial planning and information gap analysis. Northwest National Marine Renewable Energy Center Report no. 2. Corvallis: NNMREC. 26 p.

Thomas, A.C. and Weatherbee, R.A. (2006) Satellite-measured temporal variability of the Columbia River plume. Remote Sensing of Environment 100:167–178.

Venegas, R.M., Strub, P.T., Beier, E., Letelier, R., Thomas, A.C., Cowles, T., James, C., Soto-Mardones, L., and Cabrera, C. (2008) Satellite-derived variability in chlorophyll, wind stress, sea surface height, and temperature in the northern California Current System. Journal of Geophysical Research 113, C03015, doi:10.1029/2007JC004481.

Ware, D.M., and Thomson, R.E. (2005) Bottom-Up Ecosystem Trophic Dynamics Determine Fish Production in the Northeast Pacific. Science 308:1280–1284.

Zamon, J.E., Phillips, E.M. and Guy, T.J. (2014) Marine bird aggregations associated with the tidally-driven plume and plume fronts of the Columbia River. Deep-Sea Research II 107:85–89.

Department of the Interior (DOI)

The Department of the Interior protects and manages the Nation's natural resources and cultural heritage; provides scientific and other information about those resources; and honors the Nation’s trust responsibilities or special commitments to American Indians, Alaska Natives, and affiliated island communities.

Bureau of Ocean Energy Management (BOEM)

The mission of the Bureau of Ocean Energy Management is to manage development of U.S. Outer Continental Shelf energy and mineral resources in an environmentally and economically responsible way.

BOEM Environmental Studies Program

The mission of the Environmental Studies Program is to provide the information needed to predict, assess, and manage impacts from offshore energy and marine mineral exploration, development, and production activities on human, marine, and coastal environments. The proposal, selection, research, review, collaboration, production, and dissemination of each of BOEM’s Environmental Studies follows the DOI Code of Scientific and Scholarly Conduct, in support of a culture of scientific and professional integrity, as set out in the DOI Departmental Manual (305 DM 3).